⌘ *Author's Choice*

THE JOURNAL OF BIOLOGICAL CHEMISTRY VOL. 284, NO. 8, pp. 5186–5194, February 20, 2009

Functional Ryanodine Receptors in the Plasma Membrane of RINm5F Pancreatic β-Cells*[S]

Received for publication, July 22, 2008, and in revised form, December 11, 2008 Published, JBC Papers in Press, December 30, 2008, DOI 10.1074/jbc.M805587200

Christian Rosker, Gargi Meur[1], Emily J. A. Taylor[1], and Colin W. Taylor[2]

From the Department of Pharmacology, University of Cambridge, Cambridge CB2 1PD, United Kingdom

Ryanodine receptors (RyR) are Ca^{2+} channels that mediate Ca^{2+} release from intracellular stores in response to diverse intracellular signals. In RINm5F insulinoma cells, caffeine, and 4-chloro-*m*-cresol (4CmC), agonists of RyR, stimulated Ca^{2+} entry that was independent of store-operated Ca^{2+} entry, and blocked by prior incubation with a concentration of ryanodine that inactivates RyR. Patch-clamp recording identified small numbers of large-conductance (γ_K = 169 pS) cation channels that were activated by caffeine, 4CmC or low concentrations of ryanodine. Similar channels were detected in rat pancreatic β-cells. In RINm5F cells, the channels were blocked by cytosolic, but not extracellular, ruthenium red. Subcellular fractionation showed that type 3 IP_3 receptors (IP_3R3) were expressed predominantly in endoplasmic reticulum, whereas RyR2 were present also in plasma membrane fractions. Using RNAi selectively to reduce expression of RyR1, RyR2, or IP_3R3, we showed that RyR2 mediates both the Ca^{2+} entry and the plasma membrane currents evoked by agonists of RyR. We conclude that small numbers of RyR2 are selectively expressed in the plasma membrane of RINm5F pancreatic β-cells, where they mediate Ca^{2+} entry.

Ryanodine receptors (RyR)[3] and inositol 1,4,5-trisphosphate receptors (IP_3R) (1, 2) are the archetypal intracellular Ca^{2+} channels. Both are widely expressed, although RyR are more restricted in their expression than IP_3R (3, 4). In common with many cells, pancreatic β-cells and insulin-secreting cell lines express both IP_3R (predominantly IP_3R3) (5, 6) and RyR (predominantly RyR2) (7). Both RyR and IP_3R are expressed mostly within membranes of the endoplasmic (ER), where they mediate release of Ca^{2+}. Functional RyR are also expressed in the secretory vesicles (8, 9) or, and perhaps more likely, in the endosomes of β-cells (10). Despite earlier suggestions (11), IP_3R are probably not present in the secretory vesicles of β-cells (8, 12, 13).

All three subtypes of IP_3R are stimulated by IP_3 with Ca^{2+} (1), and the three subtypes of RyR are each directly regulated by Ca^{2+}. However, RyR differ in whether their most important physiological stimulus is depolarization of the plasma membrane (RyR1), Ca^{2+} (RyR2) or additional intracellular messengers like cyclic ADP-ribose. The latter stimulates both Ca^{2+} release and insulin secretion in β-cells (8, 14). The activities of both families of intracellular Ca^{2+} channels are also modulated by many additional signals that act directly or via phosphorylation (15, 16). Although they commonly mediate release of Ca^{2+} from the ER, both IP_3R and RyR select rather poorly between Ca^{2+} and other cations (permeability ratio, P_{Ca}/P_K ~7) (1, 17). This may allow electrogenic Ca^{2+} release from the ER to be rapidly compensated by uptake of K^+ (18), and where RyR or IP_3R are expressed in other membranes it may allow them to affect membrane potential.

Both Ca^{2+} entry and release of Ca^{2+} from intracellular stores contribute to the oscillatory increases in cytosolic Ca^{2+} concentration ($[Ca^{2+}]_i$) that stimulate exocytosis of insulin-containing vesicles in pancreatic β-cells (7). Glucose rapidly equilibrates across the plasma membrane (PM) of β-cells and its oxidative metabolism by mitochondria increases the cytosolic ATP/ADP ratio, causing K_{ATP} channels to close (19). This allows an unidentified leak current to depolarize the PM (20) and activate voltage-gated Ca^{2+} channels, predominantly L-type Ca^{2+} channels (21). The resulting Ca^{2+} entry is amplified by Ca^{2+}-induced Ca^{2+} release from intracellular stores (7), triggering exocytotic release of insulin-containing dense-core vesicles (22). The importance of this sequence is clear from the widespread use of sulfonylurea drugs, which close K_{ATP} channels, in the treatment of type 2 diabetes. Ca^{2+} uptake by mitochondria beneath the PM further stimulates ATP production, amplifying the initial response to glucose and perhaps thereby contributing to the sustained phase of insulin release (23). However, neither the increase in $[Ca^{2+}]_i$ nor the insulin release evoked by glucose or other nutrients is entirely dependent on Ca^{2+} entry (7, 24) or closure of K_{ATP} channels (25). This suggests that glucose metabolism may also more directly activate RyR (7, 26) and/or IP_3R (27) to cause release of Ca^{2+} from intracellular stores. A change in the ATP/ADP ratio is one means whereby nutrient metabolism may be linked to opening of intracellular Ca^{2+} channels because both RyR (28) and IP_3R (1) are stimulated by ATP.

The other major physiological regulators of insulin release are the incretins: glucagon-like peptide-1 and glucose-dependent insulinotropic hormone (29). These hormones, released by

* This work was supported by the Wellcome Trust and the Biotechnology and Biological Sciences Research Council (UK). The costs of publication of this article were defrayed in part by the payment of page charges. This article must therefore be hereby marked "*advertisement*" in accordance with 18 U.S.C. Section 1734 solely to indicate this fact.

[S] The online version of this article (available at http://www.jbc.org) contains supplemental Tables S1–S6.

⌘ *Author's Choice*—Final version full access.

[1] Both authors contributed equally.

[2] To whom correspondence should be addressed. Tel.: 44-1223-334058; E-mail: cwt1000@cam.ac.uk.

[3] The abbreviations used are: RyR, ryanodine receptor; BS, bath solution; $[Ca^{2+}]_i$, free intracellular Ca^{2+} concentration; 4CmC, 4-chloro-*m*-cresol; ER, endoplasmic reticulum; γ, single channel slope conductance; HBS, Hepes-buffered saline; IP_3R, inositol 1,4,5-trisphosphate receptor; PBS, phosphate-buffered saline; PM, plasma membrane; P_o, single channel open probability; PS, pipette solution.

cells in the small intestine, stimulate synthesis of cAMP in β-cells and thereby potentiate glucose-evoked insulin release (30). These pathways are also targets of drugs used successfully to treat type 2 diabetes (29). The responses of β-cells to cAMP involve both cAMP-dependent protein kinase and epacs (exchange factors activated by cAMP) (31, 32). The effects of the latter are, at least partly, due to release of Ca^{2+} from intracellular stores via RyR (33–35) and perhaps also via IP_3R (36). The interplays between Ca^{2+} and cAMP signaling generate oscillatory changes in the concentrations of both messengers (37). RyR and IP_3R are thus implicated in mediating responses to each of the major physiological regulators of insulin secretion: glucose and incretins.

Here we report that in addition to expression in intracellular stores, which probably include both the ER and secretory vesicles and/or endosomes, functional RyR2 are also expressed in small numbers in the PM of RINm5F insulinoma cells and rat pancreatic β-cells.

EXPERIMENTAL PROCEDURES

Cell Culture—RINm5F cells were cultured at 37 °C in humidified air containing 5% CO_2 in RPMI 1640 medium containing L-glutamine (2 mM), fetal calf serum (10%), Hepes (1 mM), and 2-mercaptoethanol (50 μM). Cells were passaged every 3–4 days when confluent.

Isolation of Rat Pancreatic β-Cells—Pancreatic β-cells were isolated from 3-week-old, male Wistar rats by Dr. Noel Smith (Department of Clinical Biochemistry) (38). Briefly, the pancreas was perfused with Hank's balanced salt solution (HBSS, Sigma) containing collagenase P (1 mg/ml, Roche), excised and incubated at 37 °C for 15 min. The islets were then washed in cold HBSS (600 × *g*, 5 min) and purified using a Histopaque discontinuous gradient (Histopaque, 1.077 g/ml; Histopaque 1, 1.119 g/ml; Sigma). Dispersed cells were resuspended in RPMI medium and allowed to attach to poly-D-ornithine-coated Petri dishes for patch-clamp recordings from isolated cells.

Subcellular Fractionation—Confluent cells (1.2×10^6 cells) were washed twice with ice-cold phosphate-buffered saline (PBS: 136.9 mM NaCl, 2.7 mM KCl, 1.5 mM KH_2PO_4, 7.7 mM Na_2HPO_4, pH 7.4), scraped into 5 ml of the same medium, centrifuged (650 × *g*, 5 min) and resuspended in 850 μl of 0.3 M sucrose supplemented with Hepes (10 mM, pH 7.4), benzamidine (1 mM), NaN_3 (2 mM), protease inhibitors (1 Roche Applied Science complete protease inhibitor mini-tablet/10 ml) and dithiothreitol (5 mM). After homogenization (15 strokes in a Dounce homogenizer) and then passage through a 25-gauge needle (30 times), the homogenate was centrifuged (1000 × *g*, 10 min, to give pellet (P1) and supernatant (S1) fractions). The supernatant was then re-centrifuged (12,000 × *g*, 10 min, to give P2 and S2). Sucrose media were prepared in 100 mM KCl, 5 mM $MgCl_2$, 100 mM imidazole, pH 6.8. Layers of 8.5% (1 ml), 40% (1.5 ml) and 60% (1.5 ml) sucrose were successively layered beneath 750 μl of the S2 supernatant fraction. The gradient was centrifuged (100,000 × *g*, 2 h, Beckman Coulter SW55T rotor), and fractions (0.25 ml, 1–19) were collected from the top of the gradient.

RNAi-mediated Knockdown of RyR1, RyR2, and IP_3R3—Cells (5×10^5 cells/well) grown in 6-well plates for 2 days were transfected using Lipofectamine RNAimax with a mixture of two RNAi for either RyR1, RyR2 (10 nM each, Invitrogen), or IP_3R3 (10 nM, Qiagen). After 36–48 h, cells were re-seeded (5×10^5 cells/well) and after a further 48 h transfected again with the same RNAi mixture. Cells were used 48–60 h after the second transfection. The RNAi used are listed in supplemental Table S1.

Immunoblotting and Protein Assays—Cells (3 × 35-mm dishes) were washed twice in PBS and lysed (PBS with 1% Triton X-100). Protein concentrations were measured using the Quant-iT protein assay kit (Invitrogen). After SDS-PAGE (3–8%, Invitrogen NuPAGE), proteins were transferred to a polyvinylidene difluoride membrane using an iBLOT apparatus (Invitrogen) and incubated with primary antibody. The antibodies used were: monoclonal IP_3R3 (Transduction Laboratories, 1:1000), RyR2 (Calbiochem, 1:1000), rabbit RyR1 (39) (1:1000), plasma membrane Ca^{2+}-ATPase (Alexis, 1:1000) and rabbit polyclonal calnexin (Santa Cruz Biotechnology, 1:500). The blots were then incubated with horseradish peroxidase-conjugated donkey anti-rabbit (AbCam, 1:5000) or goat anti-mouse (Promega, 1:5000) secondary antiserum and visualized with SuperSignal West Pico chemiluminescent substrate (Pierce). Bands were quantified using GeneTools software (Syngene).

Quantitative PCR—Total RNA was isolated from cell lysates and reverse transcribed into cDNA (20 μl) using a fast lane cDNA direct kit (Qiagen). QPCR was performed on a Rotor-Gene 6000 (Corbett Research) in a final volume of 15 μl using Sensimix Plus SYBR master mix (Quantace), 0.5 μM actin primer or Quantitect primers for IP_3R1–3 and RyR1–3, and 0.4 μl cDNA. Primers are listed in supplemental Table S2. QPCR conditions were: initial denaturation at 95 °C for 10 min, followed by 40 cycles at 95 °C for 10 s and 60 °C for 30 s. After the last cycle, a melting curve was performed to confirm the identity of the amplified product. Data were analyzed using quantification software supplied with Rotorgene 6000 (40).

Single Channel Recording—Cells attached to uncoated plastic Petri dishes were rinsed with, and then incubated in, bath solution (BS) containing 140 mM cesium methanesulfonate, 10 mM Hepes, 500 μM BAPTA, 270 μM $CaCl_2$ (free $[Ca^{2+}] = 246$ nM), pH 7.1. Where indicated, cesium methanesulfonate was iso-osomotically replaced by KCl, NaCl, Tris-HCl or *N*-methyl D-glucamine-HCl. Pipettes were pulled from borosilicate glass and had resistances of 10–30 MΩ when filled with pipette solution (PS). Most recordings were performed with symmetrical solutions. Currents were recorded with an Axopatch 200B amplifier using pClamp 9.0, digitized at 10 kHz and filtered at 1 kHz. Capacitative currents were cancelled before recording. Single channel currents were recorded in the cell-attached or inside-out configuration of the patch-clamp technique. All recordings were performed at room temperature. Currents were analyzed using pClamp 9.0 software.

Measurements of $[Ca^{2+}]_i$ and Mn^{2+} Entry—Cells cultured on 22-mm round glass coverslips were incubated with Fura 2AM (2 μM prepared in anhydrous DMSO) in HBS supplemented with probenecid (2.5 mM) and Pluronic F127 (0.02%) for 45 min at 20 °C, followed by a further 45-min incubation to allow de-esterification of the indicator. HBS had the following

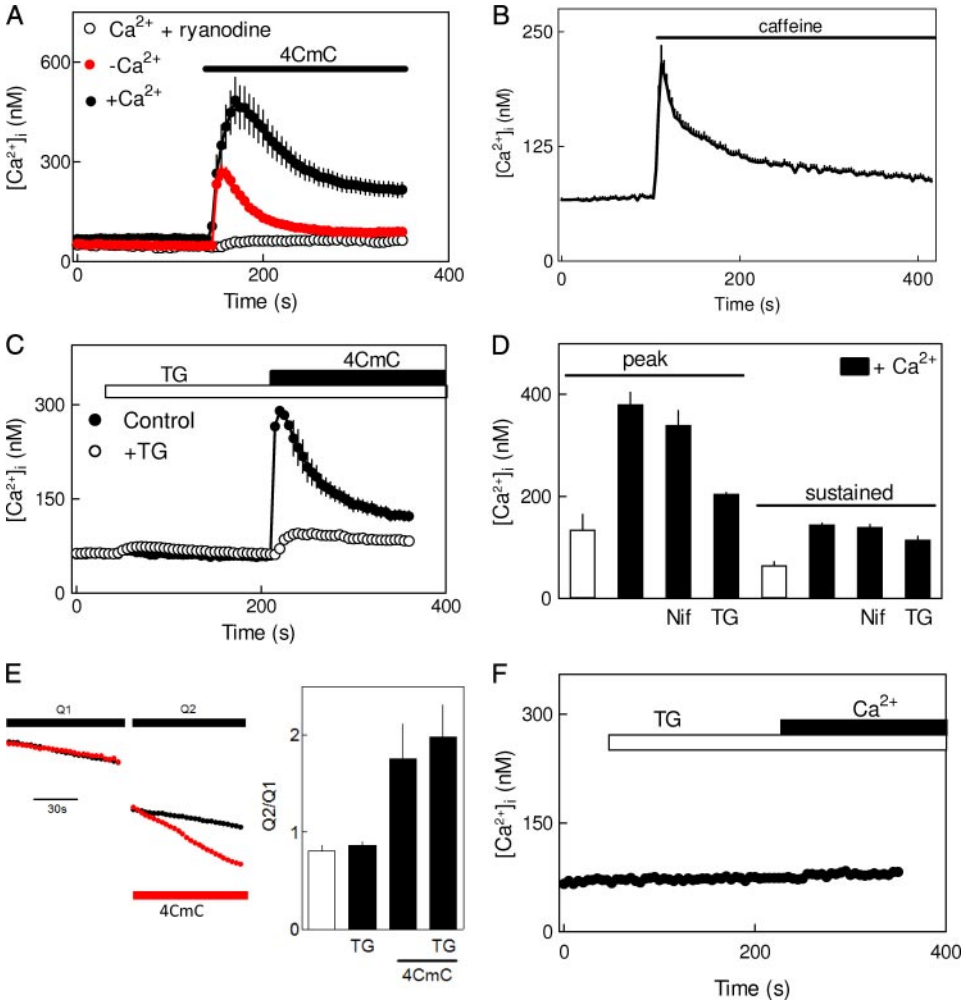

FIGURE 1. **Ca^{2+} entry evoked by agonists of RyR.** *A*, Ca^{2+} signals evoked by 4CmC (1 mM) in HBS with or without extracellular Ca^{2+} and after pretreatment with ryanodine (400 μM, 30 min). Traces (here and in subsequent panels) show the responses from ~50 individual cells taken from at least three independent experiments (means ± S.E., but with many error bars smaller than the symbols). *B*, responses to caffeine (1 mM) in normal HBS. *C*, Ca^{2+} signals evoked by 4CmC (1 mM) in Ca^{2+}-free medium alone or after pretreatment with thapsigargin (*TG*, 1 μM). *D*, peak (after ~30 s) and sustained (after 200 s) changes in $[Ca^{2+}]_i$ evoked by 4CmC in the absence (*open bars*) and presence of extracellular Ca^{2+}, and the latter after pretreatment (2 min) with nifedipine (*Nif*, 10 μM) or thapsigargin (1 μM). *E*, Mn^{2+} entry (0.5 mM) was measured by quenching of Fura 2 fluorescence in control cells (*Q1*). Mn^{2+} was then removed and the cells incubated with thapsigargin (1 μM) for 5 min (during the break between the traces) before again measuring Mn^{2+} entry (*Q2*) in the presence of thapsigargin alone (*black*) or with 4CmC (1 mM, *red*). Typical traces are shown. Summary data show the slope of the fluorescence change during the second addition of Mn^{2+} (Q2, with the stimulus) as a % (Q2/Q1) of the slope recorded during the first addition (Q1, without stimulus). Results are means ± S.E., n = 30–61. *F*, restoration of extracellular Ca^{2+} (1.5 mM) to cells pretreated with thapsigargin (1 μM) in Ca^{2+}-free HBS fails to evoke Ca^{2+} entry.

composition: 135 mM NaCl, 5.9 mM KCl, 1.2 mM $MgCl_2$, 11.6 mM Hepes, 11.5 mM glucose, and 1.5 mM $CaCl_2$ (replaced by 1 mM EGTA in Ca^{2+}-free HBS), pH 7.3. Fluorescence ratios (excitation at 340 and 380 nm; emission at 510 nm) from single cells were collected at 20 °C at 5-s intervals. After correction for autofluorescence (by addition of 1 μM ionomycin with 10 mM $MnCl_2$), fluorescence ratios were calibrated to $[Ca^{2+}]_i$ using a look-up table created from standard Ca^{2+} solutions (Molecular Probes).

Quenching of fura 2 fluorescence by Mn^{2+} entry was measured in similarly loaded cells bathed in Ca^{2+}-free HBS supplemented with 0.5 mM $MnCl_2$ and with fluorescence recorded after excitation at 360 nm. For all experiments, a basal rate of quench (Q1) was measured before stimulation, and the rate was again measured after stimulation (Q2). The duration of the exposure to $MnCl_2$ (100 s) was chosen to ensure that rates of Fura 2 quenching were linear during both assay periods. The effects of stimuli on rates of Mn^{2+} entry are reported as a Q2/Q1 ratio, with the ratio uniquely determined for each single cell (see Fig. 1*E*).

Materials—Fura 2AM and all culture media, except serum (Sigma), were from Invitrogen. All other reagents, including ryanodine, caffeine, 4CmC, and ruthenium red, were from Sigma.

RESULTS AND DISCUSSION

Ca^{2+} Entry Evoked by Agonists of RyR—In single cell measurements of $[Ca^{2+}]_i$ in RINmF5 insulinoma cells, most cells responded to caffeine (1 mM) or 4-chloro-*m*-cresol (4CmC, 1 mM) with a substantial increase in $[Ca^{2+}]_i$ (Fig. 1, *A* and *B*). A lower concentration of 4CmC (0.5 mM), sufficient to activate RyR1 and RyR2, but not RyR3 (41), evoked a similar sustained Ca^{2+} signal ($\Delta[Ca^{2+}]_i$ = 275 ± 18 and 176 ± 11 nM, for 1 mM and 0.5 mM 4CmC, respectively). Treatment with a high, inactivating concentration of ryanodine (400 μM) evoked no Ca^{2+} signal itself, but abolished the subsequent response to 4CmC (Fig. 1*A*). Although each stimulus was effective in the absence of extracellular Ca^{2+}, both the peak amplitude and sustained responses were substantially attenuated in Ca^{2+}-free medium (Fig. 1, *A*–*D*).

Pretreatment of cells in Ca^{2+}-free medium with thapsigargin (1 μM, 2 min) to empty the intracellular Ca^{2+} stores that express the SR/ER Ca^{2+}-ATPase (SERCA) massively reduced the 4CmC-evoked increase in $[Ca^{2+}]_i$, but without abolishing it (Fig. 1*C*). The small residual Ca^{2+} release is probably mediated by RyR in either secretory vesicles (8, 9) or endosomes (10), both of which can accumulate Ca^{2+} by mechanisms that do not require SERCA (8, 9). Quenching of fura 2 fluorescence evoked by unidirectional Mn^{2+} entry across the PM was also stimulated by 4CmC (Fig. 1*E*). These results establish that in RINm5F cells, agonists of RyR stimulate both release of intracellular Ca^{2+} stores (from both ER and secretory vesicles or endosomes) and Ca^{2+} entry. Others have also reported that agonists of RyR evoke Ca^{2+} release and Ca^{2+} entry in both β-cells and insulinoma cells (20, 42).

In most cells, emptying of intracellular Ca^{2+} stores evokes store-operated Ca^{2+} entry (SOCE) across the PM, although SOCE is perhaps less widely expressed in electrically excitable cells (43). Thapsigargin (1 μM) did not cause a substantial increase in $[Ca^{2+}]_i$, but it clearly emptied intracellular stores because it almost abolished the Ca^{2+} release evoked by 4CmC (Fig. 1*C*). However, thapsigargin caused no detectable Ca^{2+} entry. The small responses to thapsigargin were similar in the presence and absence of extracellular Ca^{2+} (not shown), and restoration of extracellular Ca^{2+} to thapsigargin-treated cells failed to evoke a Ca^{2+} signal (Fig. 1*F*). Under similar conditions, the same stocks of thapsigargin stimulated both Ca^{2+} release and SOCE in HEK cells (not shown). Furthermore, prior-treatment of RINm5F cells with thapsigargin neither evoked unidirectional Mn^{2+} entry nor affected the Mn^{2+} entry evoked by 4CmC (Fig. 1*E*). We conclude that depletion of intracellular Ca^{2+} stores fails to evoke significant SOCE in RINm5F cells. The lack of detectable SOCE is consistent with reports from insulinoma (44) and β-cells (20, 27, 45–47) where SOCE was either very small or undetectable.

Although agonists of RyR evoke Ca^{2+} release (Fig. 1, *B* and *C*) and SOCE is apparently absent from RINm5F cells (Fig. 1, *E* and *F*), both the initial and sustained responses to caffeine (not shown) or 4CmC (Fig. 1*D*) were substantially reduced in the absence of extracellular Ca^{2+}. Blocking voltage-gated L-type Ca^{2+} channels with nifedipine (10 μM) had no significant effect on either the peak or sustained responses to 4CmC, and nor had thapsigargin any effect on the sustained Ca^{2+} signals evoked by 4CmC (Fig. 1*D*).

Depolarization with 25 mM KCl (by replacement of NaCl) caused an increase in $[Ca^{2+}]_i$ (by 291 ± 12 nM, $n = 48$) that was substantially blocked (~60%) by 10 μM nifedipine (not shown). Under these depolarizing conditions and with nifedipine (10 μM) present, 4CmC (1 mM) evoked a further increase in $[Ca^{2+}]_i$ of 169 ± 21 nM ($n = 46$). The latter suggests that although 4CmC may lead to some activation of L-type Ca^{2+} channels (note the small, but statistically insignificant, inhibition of the peak 4CmC-evoked Ca^{2+} signal by nifedepine in Fig. 1*D*), these channels can mediate no more than a very small component of the 4CmC-evoked Ca^{2+} signal.

The results so far establish that agonists of RyR evoke Ca^{2+} (or Mn^{2+}) entry that is independent of SOCE or voltage-gated Ca^{2+} channels. Another study also showed that a RyR-selective agonist stimulates Ca^{2+} entry via a SOCE-independent pathway in β-cells, although it speculated that it resulted from RyR-mediated release of Ca^{2+} from a non-ER store causing activation of Ca^{2+}-permeable TRP (transient receptor potential) channels in the PM (20). Our subsequent experiments show that the Ca^{2+} entry is mediated directly by RyR in the PM.

Differential Distributions of RyR and IP_3R—The quantitative PCR (QPCR) analysis shown in supplemental Table S3 and the immunoblots shown in Fig. 2*A*, establish that RyR2 and IP_3R3 are the major intracellular Ca^{2+} channels in RINm5F cells. These results are consistent with previous reports demonstrating that IP_3R3 (5, 14, 48) and RyR2 (7, 9, 14, 33, 49) are the major subtypes of intracellular Ca^{2+} channels in pancreatic β-cells (5, 14, 33, 48, 49) and RINm5F cells (5, 6, 14, 48). Our results are also consistent with evidence showing low-level expression of

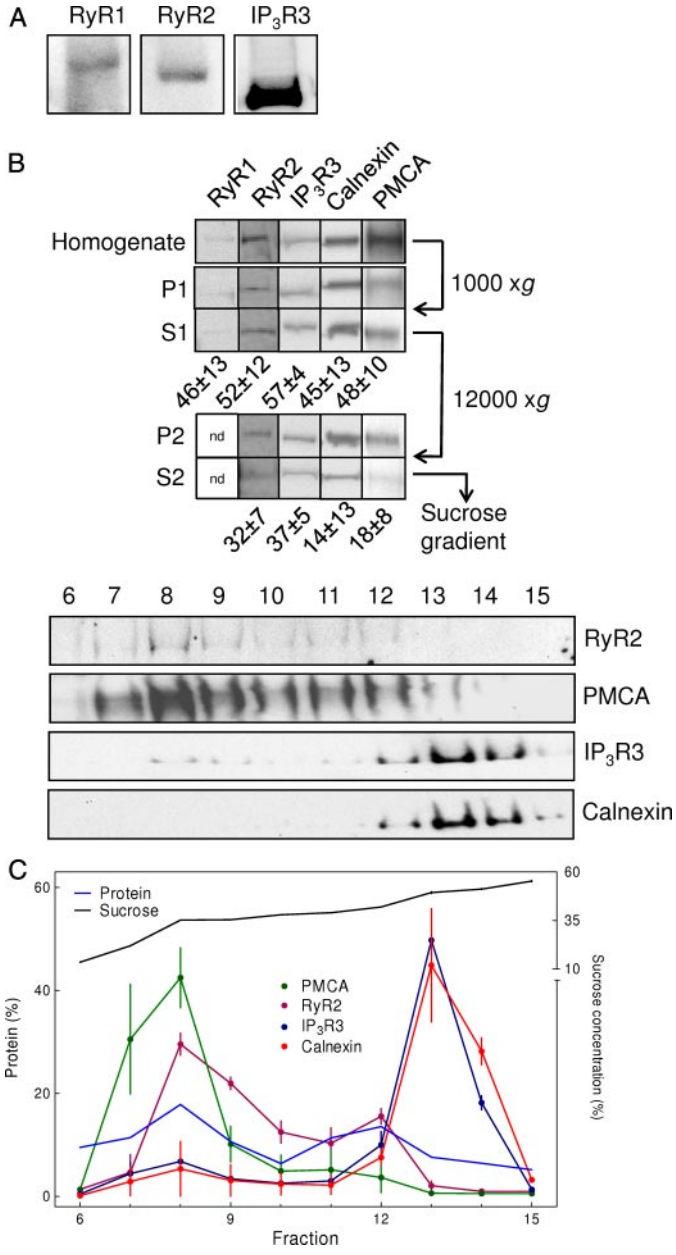

FIGURE 2. **Expression of RyR2 in RINm5F cells.** *A*, Western blots (60 μg protein/lane) from RINm5F cells stained with the indicated antibodies (typical of at least 3 blots). *B*, homogenate of RINm5F cells (see "Experimental Procedures") was subjected to two centrifugation steps (as shown) and from each supernatant (*S*) and pellet (*P*), material equivalent to the same number of cells was analyzed by Western blotting. The distribution of each protein within the supernatant fraction is shown *beneath* each gel (mean ± S.E., $n = 3$). The low level of expression of RyR1 (supplemental Table S3) prevented reliable quantification of its distribution after the first centrifugation step. The S2 supernatant was further analyzed on a discontinuous sucrose gradient, and fractions (0.25 ml, 1–19) were analyzed by Western blotting. A typical blot is shown. *C*, The distribution of proteins between fractions (means ± S.E., $n = 3$–6) is shown as a percentage of that detected in fractions 6–15 (none of the proteins were detected in the other fractions).

RyR1 (9, 14, 33) and with the lack of evidence that β-cells or insulinoma cells express RyR3 (9).

IP_3R3 and RyR2 were similarly distributed between the supernatant and pellet fractions after crude fractionation (Fig. 2*B*). Although these simple analyses failed to separate PM and ER membranes, the results are consistent with the substantial presence of IP_3R3 and RyR2 within intracellular Ca^{2+} stores.

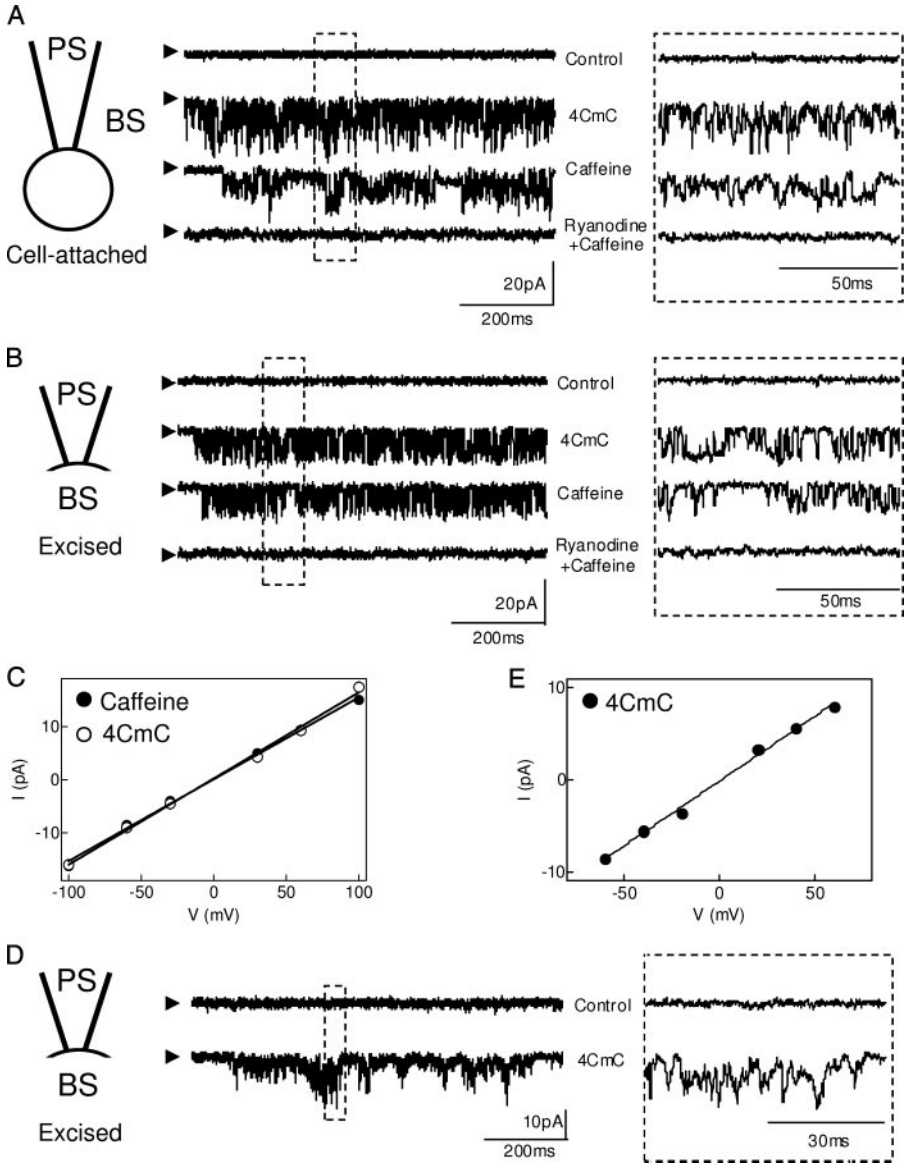

FIGURE 3. **Caffeine and 4CmC activate the same large-conductance channels in the plasma membrane of RINm5F cells and pancreatic β-cells.** *A* and *B*, cell-attached (*A*) and excised patch (*B*) recordings from RINm5F cells with cesium methanesulfonate in both BS and PS at a holding potential of −100 mV. Caffeine (1 mM) or 4CmC (1 mM) were included in BS as indicated. In the *bottom trace* of each panel, cells were preincubated with ryanodine (400 μM, 30 min) before stimulating with caffeine. Traces are representative of ≥ 5 (n = 2 for ryanodine) independent experiments (see "Results and Discussion"). *Arrows* denote closed state. For each recording, the *boxed area* is shown on an expanded timescale on the *right*. *C*, current-voltage relationship for channels activated by caffeine and 4CmC. Results are means ± S.E. n = 6–9 (most error bars are smaller than the symbols). *D*, typical excised patch recording from a rat pancreatic β-cell with cesium methanesulfonate in both BS and PS, at a holding potential of −40 mV, and with 4CmC (1 mM) included in BS as indicated. The *boxed area* is shown on an expanded timescale on the right. *E*, corresponding current-voltage relationship for β-cells (means ± S.E., n = 5).

However, sucrose-gradient centrifugation of a fraction (*S2* in Fig. 2*B*) that included 20% of all IP_3R3 and RyR2, clearly separated PM from ER, and IP_3R3 from RyR2. IP_3R3 appeared in the same fractions as calnexin, an integral ER protein, whereas RyR2 was concentrated in the same fractions as the plasma membrane Ca^{2+}-ATPase (PMCA, Fig. 2, *B* and *C*). These results do not prove that RyR2 are expressed in the PM, but they strongly suggest that at least some RyR2 are expressed in a different membrane compartment to IP_3R3.

Plasma Membrane Channels Activated by Agonists of RyR—In cell-attached patch-clamp recordings from RINm5F cells with cesium methansulphonate in both the bathing solution (BS) and pipette solution (PS), concentrations of 4CmC (1 mM) or caffeine (1 mM) typical of those used to activate RyR (41) stimulated channel activity (Fig. 3*A*). Pre-incubation (30 min) with a high concentration (400 μM) of ryanodine, sufficient to inhibit all RyR subtypes (50), abolished responses to both stimuli (Fig. 3*A*). Similar results were obtained with excised patches (Fig. 3*B*). In both sets of recordings, GΩ seals were obtained in about 50% of attempts. The frequency with which channels were detected varied between 20 and 80% in different cell preparations. It is difficult to estimate reliably the average number of channels in a patch: too many large-conductance channels may prevent formation of a GΩ seal, and patches with undetected channels will include those that failed to respond for a variety of experimental reasons. However, most active patches included one or two active channels, and very few had 3–4 channels: the average number of channels per excised patch was 1.8 ± 0.2. An analysis that assumes a random distribution of channels between patches likewise suggests the presence of ~2 channels/patch (supplemental Table S4). Assuming that our patch-clamp recordings are from ~20% of the total PM, these results suggest the presence of fewer than ~10 of these channels in the PM of each RINm5F cell. It proved impossible to achieve reliable whole cell recordings.

In symmetrical cesium methane sulfonate, the single channel slope conductance (γ) measured in cell-attached patches was the same whether they were stimulated with caffeine (γ = 147.7 ± 4.5 pS, n = 6) or 4CmC (γ = 148.3 ± 4.2 pS, n = 9) (Fig. 3*C*). We conclude that caffeine and 4CmC stimulate the same ryanodine-sensitive large-conductance cation channels in the PM of RINm5F cells.

Under similar recording conditions (symmetrical cesium methanesulphonate), 4CmC (1 mM) also activated channels in the PM of freshly isolated rat pancreatic β-cells (Fig. 3*D*). The slope conductance of the major conductance of these channels

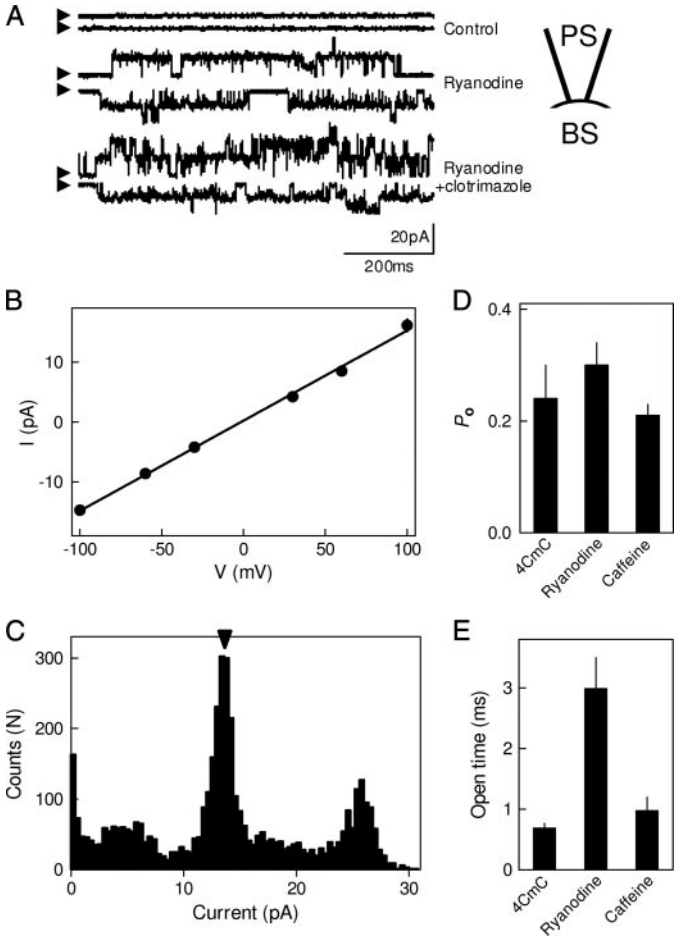

FIGURE 4. **Properties of ryanodine-activated channels in the plasma membrane.** *A,* ryanodine (4 nM) stimulates channel activity in excised patches, which is unaffected by clotrimazole (50 μM). Results show recordings in symmetrical cesium methane sulfonate at holding potentials of +80 mV (*upper trace* of each pair) and −80 mV (*lower*), each typical of ≥4 recordings. *Arrows* denote closed state. *B*, current-voltage relationship for the major conductance of the ryanodine-stimulated channels (means ± S.E., $n \geq 5$). *C*, current amplitude histogram for ryanodine-evoked currents taken from a trace similar to that shown in *A* at −80 mV. *Arrow* denotes the current level equivalent to the major single channel conductance ($\gamma = 148$ pS). *D*, *E*, P_o and mean open time (τ_o) for channels activated by ryanodine, 4CmC, and caffeine (means ± S.E., $n \geq 5$).

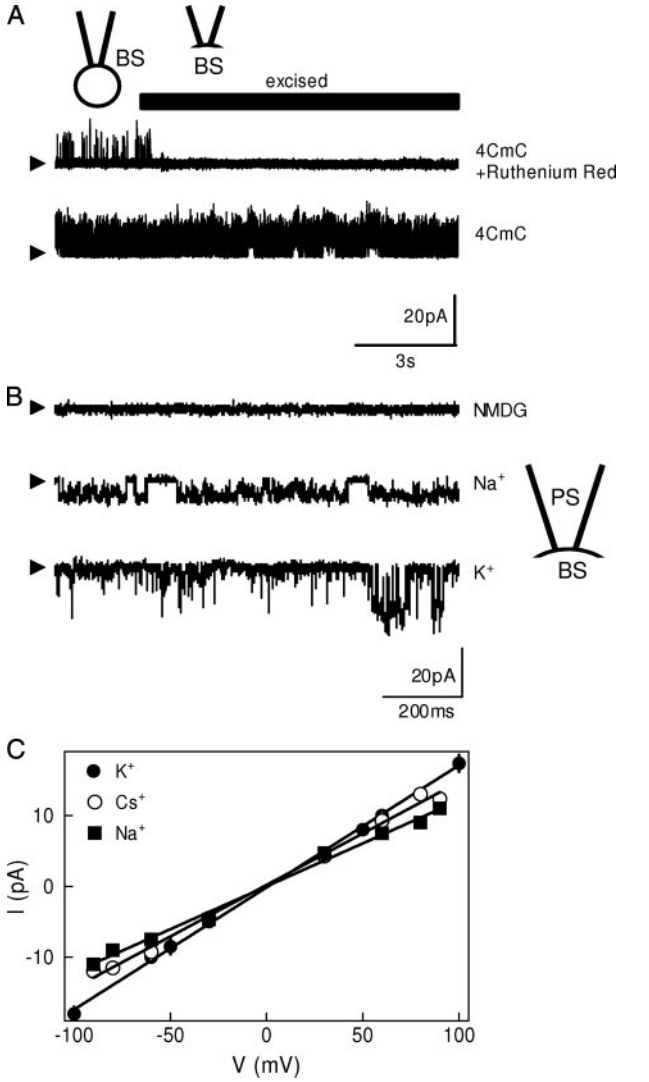

FIGURE 5. **Properties of 4CmC-activated channels in the plasma membrane.** *A*, cell-attached recordings were stimulated with 4CmC (1 mM) before excision into BS alone (*lower*) or supplemented with ruthenium red (10 μM, *upper*). Recordings were in symmetrical K^+ at +100 mV. *Arrows* denote closed state. *B*, typical recordings from excised patches held at −50 mV and stimulated with 4CmC (1 mM) in symmetrical media containing the indicated cations. *C*, current-voltage relationships from *B* (means ± S.E., $n \geq 6$, most error bars are smaller than the symbols).

($\gamma = 151.5 \pm 6.3$ pS, $n = 5$, Fig. 3*E*) was similar to that in RIN cells.

Properties of Ryanodine-activated Channels in the Plasma Membrane—In excised inside-out patches, a low concentration of ryanodine (4 nM) activated channels that were unaffected by nifedipine (10 μM, not shown) or clotrimazole (Fig. 4*A*); the latter at a concentration (50 μM) sufficient to inhibit K_{ATP} and Ca^{2+}-activated K^+ channels (51, 52). The major conductance of the ryanodine-activated channels ($\gamma_{Cs} = 147.8 \pm 3.7$ pS, $n = 7$) was the same as that of the channels activated by caffeine and 4CmC (Fig. 4*B*). The current-amplitude histograms consistently suggested the presence of minor sub-conductance states with amplitudes of ~30–50% that of the main conductance (Fig. 4*C*). Such subconductance states are common features of RyR activated by ryanodine (53). From patches with a single channel, the maximal open probability ($P_o = 0.2–0.3$) was similar for caffeine (1 mM), 4CmC (1 mM) and ryanodine (4 nM) (Fig. 4*D*), although the mean channel open time (τ_o) was significantly longer for ryanodine (Fig. 4*E*). The latter is consistent with the established ability of low concentrations of ryanodine to cause long-lasting openings of RyR (50).

Ruthenium red is an antagonist of RyR, but it is membrane-impermeant. By first activating channels with 4CmC in the cell-attached configuration and then excising the patch into BS containing ruthenium red (100 μM), we demonstrated that cytosolic ruthenium red rapidly inhibits channel activity. P_o in the cell-attached configuration was 0.25 ± 0.02 ($n = 20$), and remained at 0.24 ± 0.04 after excision into normal BS, but fell within a few seconds to 0.005 ± 0.01 after excision into BS containing ruthenium red (Fig. 5*A*). These results provide substantial further evidence that the 4CmC-activated cation channels in the PM have the properties expected of RyR.

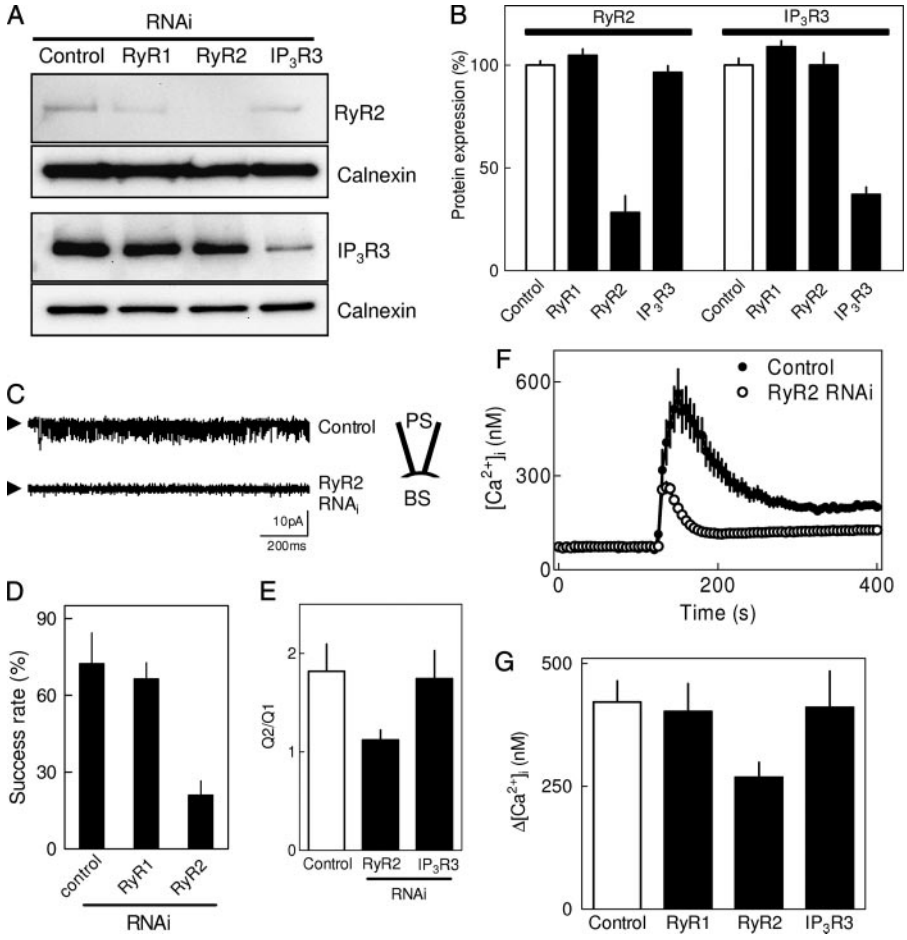

FIGURE 6. **Activation of plasma membrane cation channels and cytosolic Ca^{2+} signals requires RyR2.** *A*, Western blots showing expression of RyR2, IP_3R3, and calnexin in RINm5F cells after transfection with RNAi for RyR1, RyR2, or IP_3R3, or after mock transfection (control). The antibody to RyR1 cannot reliably detect changes in expression of endogenous RyR1, which is expressed at ~10% that of RyR2 (supplemental Table S6). *B*, summary results show expression of RyR2 and IP_3R3 derived from Western blots from four independent RNAi transfections (means ± S.E.). *C*, typical recordings (at −50 mV) from patches excised from cells after transfection with RNAi for RyR2 or mock transfection. *Arrows* denote the closed state. *D*, percentage of cells in which 4CmC (1 mM) activated channels after successful formation of a GΩ seal in cells treated with RNAi for RyR1 (n = 21), RyR2 (n = 32) or after mock transfection (control, n = 38). *E*, Mn^{2+} entry evoked by 1 mM 4CmC (with Q2/Q1 measured as in Fig. 1*E*) for cells treated with RNAi for RyR2 or IP_3R3, or after mock transfection (control). Results are means ± S.E. for 35–40 cells from two independent transfections. *F*, Ca^{2+} signals evoked by 4CmC (1 mM) in cells transfected with RNAi for RyR2 or after mock transfection (control). Results are means ± S.E., n = 47 and 32 cells, respectively. *G*, peak Ca^{2+} signals evoked by 4CmC (1 mM) in cells treated with RNAi for RyR1, RyR2, or IP_3R3, or after mock transfection (control). Means ± S.E., n = 30–76 cells.

In excised patches stimulated with 4CmC (1 mM) under symmetrical ionic conditions, the channels were permeable not only to Cs^+ (γ_{Cs} = 148.3 ± 4.2 pS, n = 9), but also to K^+ (γ_K = 169.0 ± 4.8 pS, n = 5) and Na^+ (γ_{Na} = 130.2 ± 2.1 pS, n = 4) (Fig. 5, *B* and *C*). A similar number of channels and with similar P_o was detected under each of these conditions (not shown). The channels were impermeable to *N*-methyl-D-glucamine (NMDG) chloride (Fig. 5*B*). Our attempts to measure Ba^{2+} and Ca^{2+} conductances were frustrated by resealing of membrane around the patch-pipette. We were, therefore, unable to determine the relative permeability of the PM channels for monovalent and bivalent cations. Comparison of γ for the PM channels with analyses of RyR2 reconstituted into lipid bilayers (54, 55) shows that after correction for the different ionic conditions, γ of the PM channels is consistently 3–4-fold lower than for RyR2 in bilayers (supplemental Table S5). Our previous analysis of IP_3R expressed in the PM or nuclear envelope also suggested that exactly the same channel can have very different γ when expressed in different membranes (56). We have no definitive explanation for these disparities, but for IP_3R we suggested that different membranes may selectively stabilize different sub-conductance states (56). A similar explanation may account for the different γ of RyR2 in the PM and bilayers.

We have shown that RyR2 are expressed in RINm5F cells (Fig. 2*A*) and that their distribution is consistent with a presence in the PM (Fig. 2, *B* and *C*). A variety of agonists of RyR (caffeine, 4CmC, ryanodine) activate both Ca^{2+} entry in intact cells and poorly selective large-conductance cation channels in the PM. The responses are blocked by antagonists of RyR (ryanodine, ruthenium red), but not by antagonists of other cation channels. Our final experiments use RNAi to confirm that RyR2 directly mediate these responses.

Inhibition of RyR2 Expression Inhibits Responses—Using RNAi, we selectively reduced expression of RyR1, RyR2 or IP_3R3 by >50%, without reducing expression of the non-targeted proteins (Fig. 6, *A* and *B*, and supplemental Table S6).

In excised patch-clamp recordings from mock-transfected cells or cells transfected with RNAi to RyR1, 4CmC-activated cation channels were detected in ~70% of recordings that achieved a GΩ seal, but the success rate fell to 21 ± 6% for cells treated with RNAi to RyR2 (Fig. 6, *C* and *D*). The peak Ca^{2+} signals evoked by 4CmC, which depend largely on Ca^{2+} entry (Fig. 1*D*), were also selectively attenuated by treatment with RNAi to RyR2 (Fig. 6, *F* and *G*). Likewise, the effect of 4CmC on Mn^{2+} entry was almost abolished in cells treated with RNAi to RyR2, whereas RNAi to IP_3R3 had no effect (Fig. 6*E*). We conclude that RyR2 are expressed in the PM and directly mediate Ca^{2+} entry.

Expression of Functional RyR2 in the Plasma Membrane of RINm5F Cells—We have demonstrated the expression of small numbers (~10 channels/cell) of functional RyR2 in the PM of RINm5F cells and provided more limited evidence for functional RyR in the PM of rat pancreatic β-cells. Although RyR and IP_3R are widely expressed intracellular Ca^{2+} channels, accumulating evidence suggests that the same channels may also be expressed within the PM of some cells. In B-lympho-

cytes, for example, very small numbers of functional IP_3R (2–3 IP_3R/cell) are reliably expressed in the PM, where they mediate about half the Ca^{2+} entry evoked by activation of the B-cell receptor (56, 57). IP_3R, possibly distinct from those in the ER, are also expressed in the PM of olfactory neurones (58) and ciliated epithelia (59).

Several studies have detected cation channels with large, although rather variable, conductances that are activated by agonists of RyR in the PM of different cell types. These include osteoblasts, where RyR2 are proposed to mediate extracellular Ca^{2+}-sensing (60); cardiac myocytes (61) and smooth muscle (62, 63). In each case, the density of the PM channels was very low, typically no more than ~10 channels/cell, and often just 2–3 channels/cell. None of these reports established the molecular identity of the channel and several were reluctant to conclude that it was a RyR (20, 61–63), but together they provide evidence that small numbers of RyR may be expressed in the PM of several different electrically excitable cells. Our results extend these observations to RINm5F cells and pancreatic β-cells and, more importantly, they unequivocally establish that RyR2 expressed in the PM can directly mediate Ca^{2+} entry.

These results indicate that in some cells, small numbers of IP_3R or RyR can be expressed in the PM and mediate Ca^{2+} entry. The small number of these channels is significant because both RyR and IP_3R have such large conductances (Figs. 3*C*, 4*B*, and 5*C*) that very few channels can mediate substantial Ca^{2+} entry (56).

RyR are implicated in the responses of pancreatic β-cells to glucose and incretins (see Introduction); many diabetic states are associated with a loss of RyR from β-cells (10); and the immunosuppressant, FK-506, which interacts with RyR via FKBP (64), is a major cause of post-transplantation diabetes mellitus (65). But the specific roles of RyR in β-cells are incompletely resolved (7, 10, 66). It is, however, clear that whereas both IP_3R and RyR are expressed in the ER of insulinoma cells, only RyR are expressed in secretory vesicles (8) or endosomes (10). Selective targeting of RyR (and not IP_3R) to the secretory vesicles of β-cells might therefore be one step that contributes to selective expression of small numbers of RyR in the PM.

Abundant evidence implicates RyR in mediating physiological responses of β-cells to glucose and incretins (see Introduction). Our results suggest that their involvement in these responses is likely to involve RyR within both intracellular stores and the PM, and within the latter it is likely that RyR may directly mediate Ca^{2+} entry and contribute to regulation of membrane potential. It remains unclear whether the non-ER RyR reside predominantly in endosomes or secretory vesicles (8, 10), but it is significant that their presence in either organelle suggests a dynamic relationship between exocytosis of insulin-containing vesicles and trafficking of RyR2 between intracellular organelles and the PM.

We have shown that small numbers of functional RyR2 are expressed in the PM of RINm5F insulinoma cells and rat pancreatic β-cells, where they directly mediate Ca^{2+} entry and may also regulate membrane potential. We suggest that exocytosis of insulin-containing vesicles and the subsequent retrieval of membrane by endocytosis (67) may allow dynamic regulation of RyR expression in the PM.

Acknowledgments—We thank G. Meissner for providing the antiserum for RyR1, and N. Smith and S. Ozanne for help with β-cells.

REFERENCES

1. Foskett, J. K., White, C., Cheung, K. H., and Mak, D. O. (2007) *Physiol. Rev.* **87,** 593–658
2. Hamilton, S. L. (2005) *Cell Calcium* **38,** 253–260
3. Taylor, C. W., Genazzani, A. A., and Morris, S. A. (1999) *Cell Calcium* **26,** 237–251
4. Sutko, J. L., and Airey, J. A. (1996) *Physiol. Rev.* **76,** 1027–1071
5. Blondel, O., Takeda, J., Janssen, H., Seino, S., and Bell, G. I. (1993) *J. Biol. Chem.* **268,** 11356–11363
6. Swatton, J. E., Morris, S. A., Cardy, T. J. A., and Taylor, C. W. (1999) *Biochem. J.* **344,** 55–60
7. Islam, M. S. (2002) *Diabetes* **51,** 1299–1309
8. Mitchell, K. J., Pinton, P., Varadi, A., Tacchetti, C., Ainscow, E. K., Pozzan, T., Rizzuto, R., and Rutter, G. A. (2001) *J. Cell Biol.* **155,** 41–51
9. Mitchell, K. J., Lai, F. A., and Rutter, G. A. (2003) *J. Biol. Chem.* **278,** 11057–11064
10. Johnson, J. D., Kuang, S., Misler, S., and Polonsky, K. S. (2004) *FASEB J.* **18,** 878–880
11. Blondel, O., Bell, G. I., Moody, M., Miller, R. J., and Gibbons, S. J. (1994) *J. Biol. Chem.* **269,** 27167–27170
12. Ravazzola, M., Halban, P. A., and Orci, L. (1996) *Proc. Natl. Acad. Sci. U. S. A.* **93,** 2745–2748
13. Prentki, M., Biden, T. J., Janjic, D., Irvine, R. F., Berridge, M. J., and Wollheim, C. B. (1984) *Nature* **309,** 562–564
14. Takasawa, S., Akiyama, T., Nata, K., Kuroki, M., Tohgo, A., Noguchi, N., Kobayashi, S., Kato, I., Katada, T., and Okamoto, H. (1998) *J. Biol. Chem.* **273,** 2497–2500
15. Patterson, R. L., Boehning, D., and Snyder, S. H. (2004) *Annu. Rev. Biochem.* **73,** 437–465
16. Bers, D. M. (2004) *J. Mol. Cell. Cardiol.* **37,** 417–429
17. Williams, A. J. (2002) *Front. Biosci.* **7,** 1–8
18. Gillespie, D., and Fill, M. (2008) *Biophys. J.* **95,** 3706–3714
19. Nichols, C. G. (2006) *Nature* **440,** 470–476
20. Gustafsson, A. J., Ingelman-Sundberg, H., Dzabic, M., Awasum, J., Nguyen, K. H., Ostenson, C. G., Pierro, C., Tedeschi, P., Woolcott, O., Chiounan, S., Lund, P. E., Larsson, O., and Islam, M. S. (2005) *FASEB J.* **19,** 301–303
21. Ashcroft, F. M., Proks, P., Smith, P. A., Ammala, C., Bokvist, K., and Rorsman, P. (1994) *J. Cell. Biochem.* **55 (**suppl.), 54–65
22. Bokvist, K., Eliasson, L., Ammala, C., Renstrom, E., and Rorsman, P. (1995) *EMBO J.* **14,** 50–57
23. Wiederkehr, A., and Wollheim, C. B. (2006) *Endocrinology* **147,** 2643–2649
24. Rojas, E., Carroll, P. B., Ricordi, C., Boschero, A. C., Stojilkovic, S. S., and Atwater, I. (1994) *Endocrinology* **134,** 1771–1781
25. Henquin, J. C. (2000) *Diabetes* **49,** 1751–1760
26. Shigeto, M., Katsura, M., Matsuda, M., Ohkuma, S., and Kaku, K. (2007) *J. Pharmacol. Exp. Ther.* **322,** 1–7
27. Dyachok, O., and Gylfe, E. (2004) *J. Biol. Chem.* **279,** 45455–45461
28. Kermode, H., Williams, A. J., and Sitsapesan, R. (1998) *Biophys. J.* **74,** 1296–1304
29. Drucker, D. J. (2006) *Cell Metab.* **3,** 153–165
30. Holst, J. J. (2007) *Physiol. Rev.* **87,** 1409–1439
31. Holz, G. G. (2004) *Diabetes* **53,** 5–13
32. Szaszak, M., Christian, F., Rosenthal, W., and Klussmann, E. (2007) *Cell. Signal.* **20,** 590–601
33. Holz, G. G., Leech, C. A., Heller, R. S., Castonguay, M., and Habener, J. F. (1999) *J. Biol. Chem.* **274,** 14147–14156
34. Tsuboi, T., da Silva Xavier, G., Holz, G. G., Jouaville, L. S., Thomas, A. P., and Rutter, G. A. (2003) *Biochem. J.* **369,** 287–299
35. Kang, G., Chepurny, O. G., and Holz, G. G. (2001) *J. Physiol.* **536,** 375–385
36. Gromada, J., Dissing, S., Bokvist, K., Renström, E., Frøkjaer-Jensen, J., Wulff, B. S., and Rorsman, P. (1995) *Diabetes* **44,** 767–774

37. Dyachok, O., Isakov, Y., Sagetorp, J., and Tengholm, A. (2006) *Nature* **439,** 349–352
38. Lacy, P. E., and Kostianovsky, M. (1967) *Diabetes* **16,** 35–39
39. Meissner, G., Rousseau, E., and Lai, F. A. (1989) *J. Biol. Chem.* **264,** 1715–1722
40. Warton, K., Foster, N. C., Gold, W. A., and Stanley, K. K. (2004) *Gene* **342,** 85–95
41. Fessenden, J. D., Perez, C. F., Goth, S., Pessah, I. N., and Allen, P. D. (2003) *J. Biol. Chem.* **278,** 28727–28735
42. Woolcott, O. O., Gustafsson, A. J., Dzabic, M., Pierro, C., Tedeschi, P., Sandgren, J., Bari, M. R., Nguyen, K. H., Bianchi, M., Rakonjac, M., Radmark, O., Ostenson, C. G., and Islam, M. S. (2006) *Cell Calcium* **39,** 529–537
43. Parekh, A. B., and Putney, J. W. (2005) *Physiol. Rev.* **85,** 757–810
44. Yamasaki, M., Masgrau, R., Morgan, A. J., Churchill, G. C., Patel, S., Ashcroft, S. J., and Galione, A. (2004) *J. Biol. Chem.* **279,** 7234–7240
45. Liu, Y. J., and Gylfe, E. (1997) *Cell Calcium* **22,** 277–286
46. Miura, Y., Henquin, J. C., and Gilon, P. (1997) *J. Physiol.* **503,** 387–398
47. Mears, D., Leighton, X., Atwater, I., and Rojas, E. (1999) *Cell Calcium* **25,** 59–68
48. Lee, B., Bradford, P. G., and Laychock, S. G. (1998) *J. Mol. Endocrinol.* **21,** 31–39
49. Johnson, J. D., Han, Z., Otani, K., Ye, H., Zhang, Y., Wu, H., Horikawa, Y., Misler, S., Bell, G. I., and Polonsky, K. S. (2004) *J. Biol. Chem.* **279,** 24794–24802
50. Santonastasi, M., and Wehrens, X. H. (2007) *Acta Pharma. Sin.* **28,** 937–944
51. Tian, M., Dong, M. Q., Chiu, S. W., Lau, C. P., and Li, G. R. (2006) *Br. J. Pharmacol.* **147,** 289–297
52. Welker, S., and Drews, G. (1997) *Naunyn-Shmiedeberg's Arch. Pharmacol.* **356,** 543–550
53. Fill, M., and Copello, J. A. (2002) *Physiol. Rev.* **82,** 893–922
54. Lindsay, A. R. G., Manning, S. D., and Williams, A. J. (1991) *J. Physiol.* **439,** 463–480
55. Williams, A. J., West, D. J., and Sitsapesan, R. (2001) *Quart. Rev. Biophys.* **34,** 61–104
56. Dellis, O., Dedos, S., Tovey, S. C., Rahman, T.-U., Dubel, S. J., and Taylor, C. W. (2006) *Science* **313,** 229–233
57. Dellis, O., Rossi, A. M., Dedos, S. G., and Taylor, C. W. (2008) *J. Biol. Chem.* **283,** 751–755
58. Fadool, D. A., and Ache, B. W. (1992) *Neuron* **9,** 907–918
59. Barrera, N. P., Morales, B., and Villalon, M. (2007) *Biochem. Biophys. Res. Commun.* **364,** 815–821
60. Huang, C. L., Sun, L., Fraser, J. A., Grace, A. A., and Zaidi, M. (2007) *Ann. N. Y. Acad. Sci.* **1116,** 255–270
61. Zhang, Y. A., Tuft, R. A., Lifshitz, L. M., Fogarty, K. E., Singer, J. J., and Zou, H. (2007) *Am. J. Physiol.* **293,** H2448–H2461
62. Guerrero, A., Fay, F. S., and Singer, J. J. (1994) *J. Gen. Physiol.* **104,** 375–394
63. Loirand, G., Pacaud, P., Baron, A., Mironneau, C., and Mironneau, J. (1991) *J. Physiol.* **437,** 461–475
64. Samso, M., Shen, X., and Allen, P. D. (2006) *J. Mol. Biol.* **356,** 917–927
65. Penfornis, A., and Kury-Paulin, S. (2006) *Diabetes Metab.* **32,** 539–546
66. Zhan, X., Yang, L., Yi, M., and Jia, Y. (2008) *Eur. J. Biophys.* **37,** 773–782
67. MacDonald, P. E., and Rorsman, P. (2007) *Physiology* (*Bethesda*) **22,** 113–121